Colloid Polym Sci (2009) 287:683–693
DOI 10.1007/s00396-009-2014-3

ORIGINAL CONTRIBUTION

Polymeric microcapsules with internal cavities for ultrasonic imaging: efficient fabrication and physical characterization

Rong Lu · Hongjing Dou · Yuanyuan Qiu · Dong Zhang · Kang Sun · Yuqi Zhang · Kun Sun

Received: 28 November 2008 / Revised: 15 January 2009 / Accepted: 3 February 2009 / Published online: 24 February 2009

Abstract Polymeric microcapsules are of great potential in ultrasonic imaging due to their characteristic hollow structure. Water-in-oil-in-water ($W_1/O/W_2$) double emulsion-solvent evaporation technique is a versatile strategy applicable to most hydrophobic polymers for fabricating microcapsules; however, the adjustment of the size and inner structure of resultant microcapsules have not been systematically studied until now. Here, we evaluate in detail the parameters in double emulsification and find that the W_1/O volume ratio is a pivotal parameter which controls the hollow structure of microcapsules. In addition, an appropriate concentration of emulsifier in W_2 is essential to guarantee the hollow structure as well. For quantitatively characterizing the hollow structure of microcapsules, we propose the concept of Hollow Ratio (HR) and Hollow Degree (HD) to evaluate the percent of hollow microcapsules in products and the hollow characteristic of the microcapsules. Our study demonstrates that the HR of microcapsules can vary between 25% and 98% by only adjusting the W_1/O volume ratio. The size of microcapsule has a close relationship to its HD. Moreover, the microcapsules with both single cavity and multicavities have been fabricated by altering the energy of the second emulsification. Further, acoustic studies reveal that the microcapsules with different HD display obviously different sound attenuation spectrum and resonance frequency, which demonstrates that the adjustment of hollow structure should be an effective approach to control the acoustical properties of microcapsules for ultrasonic imaging.

Keywords Double emulsion · Microcapsules · Ultrasonic imaging · PLLA

R. Lu · H. Dou · K. Sun (✉)
State Key Lab of Metal Matrix Composites, School of Materials Science and Engineering, Shanghai Jiao Tong University, Shanghai 200240, China
e-mail: ksun@sjtu.edu.cn

Y. Qiu · D. Zhang
Institute of Acoustics, Nanjing University, Nanjing 210093, China

Y. Zhang · K. Sun
Shanghai Children's Medical Center, Shanghai 200127, China

Introduction

Hollow microspheres, so-called microcapsules, have attracted considerable attention since 1970s due to their great potential in drug delivery [1–3], blood substitutes [4, 5], catalysis [6], especially in ultrasonic imaging [3, 7–10]. Modern ultrasonic contrast agents (UCAs) are clinically used to enhance B-mode images and Doppler signals decades ago [11, 12]. They primarily comprise microcapsules formulations that circulate in the intravascular compartment and are designed to enhance acoustic signals reflected from the blood pool. For microcapsules used in ultrasonic imaging, two essential aspects are the coating materials that ensure the persistence of UCAs and the filling gas in the internal cavities. To increase the stability of UCAs, many researches focus on polymers [10, 13–16] since polymeric shells are more resistant to ultrasonic than monomolecular layer of lipids or surfactants usually for stabilizing commercial UCAs such as Optison or Albunex [17, 18]. Besides, the viscoelasticity of the shell can be controlled by adjusting the chemical composition and molecular weight of the polymers [19, 20].

Until now, various techniques are available to fabricate polymeric microcapsules, including double emulsification,

spray-drying technique, and layer-by-layer assembly [21–23]. Among them, the water-in-oil-in-water ($W_1/O/W_2$) double emulsion–solvent evaporation technique was the most commonly used one, which was patented by Vrancken [24] and Jaeger [25] nearly 40 years ago and then developed by Ogawa et al. [26]. As a powerful approach for preparing polymeric microcapsules, double emulsification technique possesses three obvious merits compared to other approaches. First of all, this method is applicable to most oil-soluble polymers. It is convenient to use various polymers with different properties according to the requirement [13, 27]. Secondly, by adding functional feeds such as drugs or nanoparticles to W_1 or O, it is facile to get microcapsules with different functionalities [27, 28]. Moreover, the process includes no chemical reaction and can be accomplished under mild condition, which permits the encapsulation of active drugs or other sensitive feeds [29].

Poly(L-lactic acid) (PLLA) and its derivatives, with their outstanding biocompatibility and biodegradability, have been one kind of most used synthetic polymers in biomedical fields [19, 20, 30]. These polymers also exhibit great potential as the shell materials of UCAs, which can be proved by several reports recently [10, 13, 27]. For example, Cui et al. fabricated PLGA [13] microcapsules by double emulsion–solvent evaporation process, and evaluated their ultrasound contrast abilities in vitro by a Power-Contrast-Imaging-triggered technology, whereas the parameters during double emulsification process were not detailed discussed. Moreover, the control of size distribution of microcapsules was studied by Liu et al. They prepared uniform-sized PLA/PLGA microcapsules loading insulin by combining a Shirasu porous glass emulsification technique and a double emulsion–solvent evaporation method [27]. Considering the close relationship between the inner cavity and the encapsulated gas in microcapsules, the inner structure is anticipated of utmost importance for the acoustical properties of microcapsule-based UCAs. However, there are few reports till now on the control of inner structure of microcapsules in double emulsification process as well as the acoustic studies of microcapsules with different hollow structures.

Herein, we present detailed studies on the preparation, physical characterization, as well as acoustical behavior of PLLA microcapsules prepared by a modified double emulsification approach, with emphasis on the control and evaluation of their inner structures. For characterizing the hollow structure more quantificationally, we propose two definitions of Hollow Ratio (HR) and Hollow Degree (HD). The microcapsules prepared at different parameters are characterized in terms of size, HR, HD and sound attenuation spectrum. The relationship between preparation parameters and physical properties of resultant microcapsules are systematically discussed.

Experimental details

Materials

PLLA (M_w=208,000) was provided by Nature Works LLC. Poly(vinyl alcohol) (PVA; degree of polymerization=1,800, degree of hydrolysis=89%) was purchased from SINOPEC Shanghai Petrochemical Company Limited. Rhodamine B was purchased from Sigma–Aldrich. Other reagents were analytically pure from Sinopharm Chemical Reagent Co., Ltd.

Microcapsules fabrication

PLLA (0.5 g) was dissolved in 20 mL methylene chloride and a designed volume of deionized water was added to the polymer solution to generate the W_1/O emulsion by homogenizer (FLUKO FM200, 10G dispersing head, 20,000 rpm) for 1 min or by ultrasonic (ULTRASONICS FS-300, continuous mode, 180 W) for 1 min. The resultant W_1/O emulsion was then poured into 100 mL PVA aqueous solution with a designed concentration and homogenized at 11,000 rpm for 4 min (except for sample H6000 and A600). The resultant $W_1/O/W_2$ double emulsion was poured into 100 mL 2% isopropanol aqueous solution and stirred at room temperature for 2 h to evaporate methylene chloride. The capsules were collected by centrifugation (25 °C, 3,500 rpm, 5 min) and washed by water for one time. Afterwards, the capsules were freeze-dried for 48 h to remove the remainder of water and other solvent. The experimental parameters are listed in Table 1.

Hollow structure characterization

To clarify the inner structure of microcapsules, the shell of microcapsules were dyed by adding rhodamine B to methylene chloride during the fabrication of microcapsules. If the microparticle was hollow, bright annulus would be seen during the layer scanning of confocal microscopy [31].

Ten microliters aqueous suspension of microcapsules was placed between two glass slides and examined under LSM 510 META laser confocal scanning microscopy (LCSM) equipped with 1 mW helium neon laser, using Plan-Neofluar 40×/0.75 objective. Red fluorescence was observed with LP 560 nm emission filter under 543-nm laser illumination. The pinhole diameter was set at 125 μm.

The outer and inner radius of each capsule was measured directly on the confocal images using Zeiss software. Measurements were carried out in the equatorial plane of each capsule to minimize the error due to the position of the slice. The size of a pixel was 70 nm.

Table 1 Detailed experimental parameters of samples

Samples	The first emulsification		The second emulsification	
	W_1/O (*v*/*v*)	Approach (setup)	PVA concentration (wt.%)	Approach (setup)
HH1	0.13	H[a] (20,000 rpm)	1.0	H[a] (11,000 rpm)
HH2	0.20			
HH3	0.27			
HH4	0.33			
HH5	0.47			
HH6	0.53			
HH7	0.60			
HH8	0.67			
UH1	0.10	U[b] (180 W)		
UH2	0.20			
UH3	0.40			
UH4	0.50			
PVA10	0.40	H[a] (20,000 rpm)		
PVA05			0.5	
PVA03			0.3	
PVA02			0.2	
H6000			1.0	H[a] (6,000 rpm)
A600				A[c] (600 rpm)

[a] Homogenizer
[b] Ultrasonic
[c] Agitation

Definition of HR and HD

It is confirmed by LCSM observation that the microparticles prepared by double emulsion–solvent evaporation technique are mostly the mixture of hollow microcapsules and solid microspheres. Therefore, in order to characterize the ratio of hollow microcapsules in a product, HR is proposed as follows:

$$\mathrm{HR} = (N_\mathrm{H}/N_\mathrm{T}) \times 100\%$$

where N_H represents the amount of hollow microcapsules and N_T represents the total number of microparticles which include hollow microcapsules and solid microspheres. For each sample, N_H and N_T are determined by the morphology observation of 200 stochastic microparticles under LCSM.

R and r represent the outer and inner radius of a single microcapsule. Microcapsules with the same R may have different r inside. In order to characterize this distinction, another concept of HD is defined as:

$$\mathrm{HD} = r/R$$

So, for a solid microsphere, the value of HD is 0, while for monomolecular layer stabilized microbubble, the value of HD is 1.

Average HD for a sample can be calculated by the expression:

$$\text{Average HD} = \sum \Phi N_\Phi / N_\mathrm{T}$$

where N_Φ represents the number of microparticles (including hollow microcapsules and solid microspheres) whose HD are Φ.

Therefore, with index of HR and average HD, we can estimate the hollow structure of a sample clearly and compare different samples conveniently. In this work, the pivotal parameters which control the HR and HD of the resultant microcapsules are anticipated to be revealed.

Size measurement

Size measurements on microcapsules were performed using a particle size analyzer (Mastersizer 2000, Malvern) based on laser granulometry and volume average size (D_v) was obtained. Besides, number average size (D_n) of each sample was calculated from the outer diameter of 200 microparticles through LCSM images:

$$D_\mathrm{n} = \sum D_i/200 (i = 1,\ 2,\ 3,\ \ldots, 200)$$

Sound attenuation spectrum measurement

An ultrasound spectroscopy method [32] is used to measure the acoustic attenuation spectrum. As shown in Scheme 1, a broadband acoustic pulse is excited and the signals prior to and during insertion of the specimen are detected and analyzed by FFT software. The sound attenuation in specimen can be expressed as

$$\alpha_\mathrm{s} = \alpha_\mathrm{w} + \frac{1}{2d} \ln\left(\frac{|P_\mathrm{w}(\omega)T(\omega)|}{|P_\mathrm{w}(\omega)|}\right)$$

where α_w is the sound attenuation in water; P_w (ω) and P_s (ω) are amplitude spectra before and after the insertion of

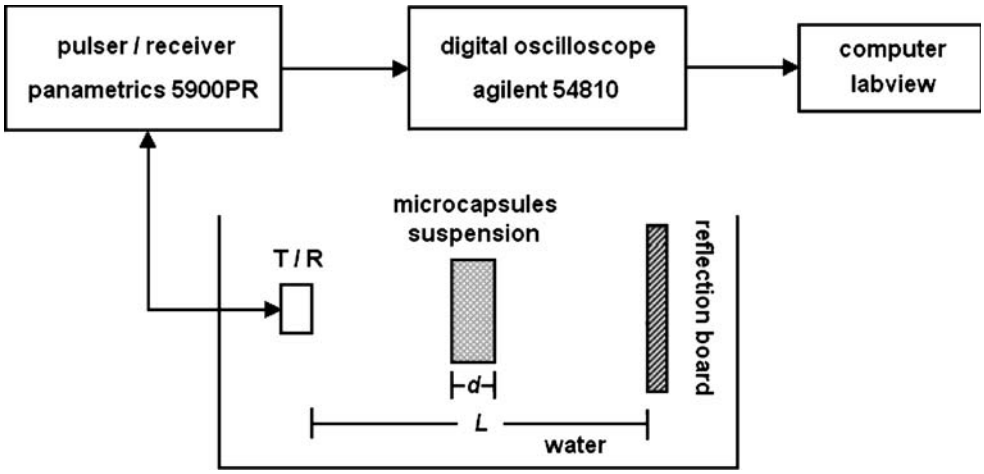

Scheme 1 Experimental setup for measuring sound attenuation spectrum

specimen respectively; $T(\omega)$ is the spectrum of the overall transmission coefficient, with the pulse signal passing through every interface twice taken into consideration; d is the thickness of specimen.

A broadband planar transducer (diameter 13 mm, center frequency 2.25 MHz, −6 dB band 1.1–3.9 MHz, Panametrics, USA) is used as both the transmitter and receiver. An aluminum plate located at a distance of L=50 mm is used to reflect the signal. A sound permeable container with a thickness of d=2 mm is inserted between the transducer and the reflective board and is about 5 mm close to the latter. A pulser or receiver (Panametrics 5900PR, USA) generates a broadband pulse signal covering frequency range from 1 kHz to 20 MHz. The pulse signal is set to be 8 μJ at a pulse repetition frequency of 1 kHz. The received signal is amplified by the pulser or receiver and recorded by a digital oscilloscope (Agilent 54810, USA) with a sampling frequency of 100 MHz/s and a sampling point number of 2,048.

Twenty-five milligrams microcapsules were dispersed in 10 mL normal saline, and the resultant suspension was poured into a sound permeable container in the water tank. The received signals were recorded before and after the insertion of the container. The sound attenuation spectrum of microcapsules suspension was the D value of the two spectra of the received signals.

Results and discussion

Before discussing the influence factors of hollow structures, it is necessary to emphasize the criteria to select the molecular weight of PLLA and the kinds of emulsifier. In our previous work, we studied the influence of the molecule weight of PLLA and different emulsifiers on the morphology of the resultant microcapsules. It was found that by using PLLA with high molecular weight (M_w=208,000) as the shell material and PVA as the emulsifier, spherical microcapsules with smooth surface could be obtained [33]. It is considered that higher molecular weight is benefit to the formation of microcapsules, which is also consistent with the result reported in the reference [14]. Therefore, PLLA with high molecular weight (M_w=208,000) and PVA are chosen as the shell material and the emulsifier, respectively, in this study.

The size and inner structure of microcapsules are two pivotal characteristic of microcapsule-based UCAs for further application. The following parts will, respectively, investigate the important experimental parameters in the first and the second emulsification [34] and try to find key points which control the size and inner structure of resultant microcapsules. Furthermore, the acoustical properties of microcapsules with different inner structures will be disclosed.

The first emulsification

The first emulsification is to obtain W_1/O emulsion. Theoretically, inner aqueous phase (W_1) and middle oil phase (O) are, respectively, the precursor of cavity and shell for the microcapsule [35]. It is considered that with a certain volume and concentration of O, the W_1/O volume ratio will consequentially influence the hollow structure of microcapsules. Therefore, a series of W_1/O volume ratio was adopted in the preparation of microcapsules. Besides, the energy of the first emulsification can directly change the size of inner aqueous droplets and then influence the size and hollow structure of resultant microcapsules. So, we designed HH and UH series experiments in which homogenizer and ultrasonic were, respectively, applied in the first emulsification.

For each sample, the outer and inner radii of 200 microparticles were measured as described in the experimental details, and then the HD of these 200 microparticles was calculated according to the definition. Finally, the number percent distribution of HD for each sample was counted. Figure 1 presents LCSM images and number

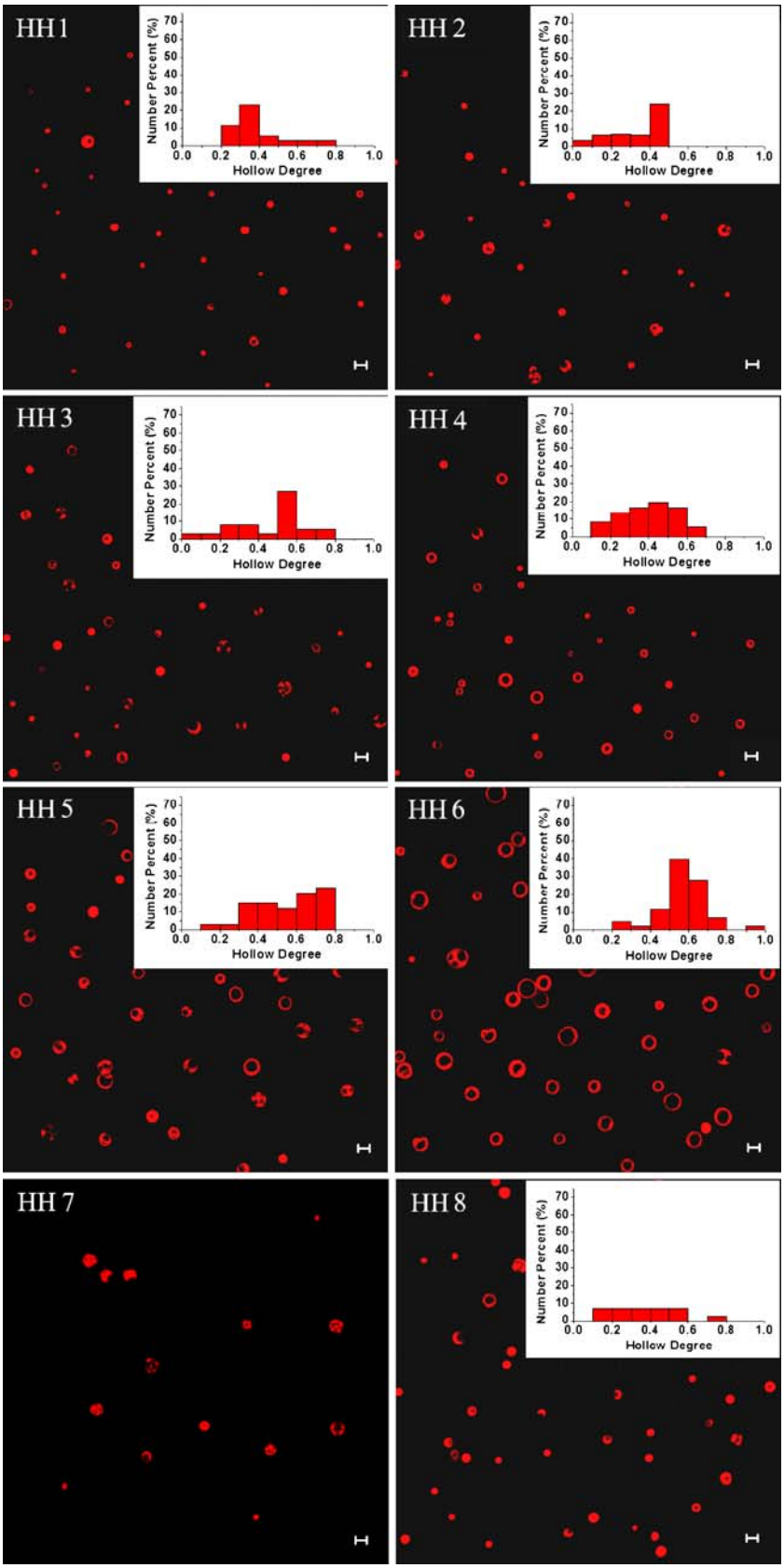

Fig. 1 LCSM images of HH series microcapsules prepared by different W_1/O volume ratios (HH represent that the first and second emulsification are all by homogenizer. The W_1/O volume ratios, for sample, *HH1* to *HH8*, are 0.13, 0.20, 0.27, 0.33, 0.47, 0.53, 0.60, and 0.67, respectively. The *insets* are number percent distributions of hollow degree. *Scale bars* represent 10 μm in all of images)

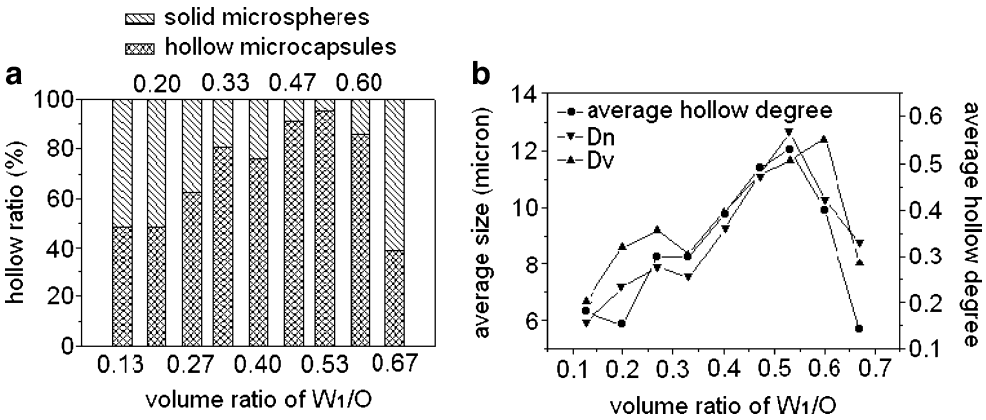

Fig. 2 **a**, **b** Influence of W_1/O volume ratio on the hollow ratio, average hollow degree and average size of microcapsules using homogenizer in the first emulsification (D_n and D_v represent the number average size calculated from LCSM images and the volume average size measured by laser granulometry, respectively)

percent distributions of HD for HH series samples (in sample HH7, many broken microcapsules made the HD measurement difficult.). With the increase of W_1/O volume ratio from 0.13 to 0.53, more and more hollow microcapsules appear in the sample, with number percent distribution of HD moves to the higher value. Further increasing the W_1/O volume ratio results in many broken microcapsules appear in LCSM images. The HR of each sample was also counted and shown in Fig. 2a. It is obvious that HR reach the peak value around the W_1/O volume ratio of 0.53 and then fall down. This result indicates that the W_1/O volume ratio plays an important role in controlling the hollow structure of microcapsules.

Figure 2b shows the average HD, D_n, and D_v of microcapsules prepared at different W_1/O volume ratios, using homogenizer in the first emulsification. Average HD and the average size display similar variational tendency, i.e., they increase first and then fall down with the increase of W_1/O volume ratio. It is considered that size and HD may have intrinsic relationship.

The size and hollow structure of UH series samples were measured and evaluated by a similar approach. For UH series samples, LCSM images and number percent distribution of HD are shown in Fig. 3, while HR, average HD, and average size are shown in Fig. 4. It is obviously displayed that the HR, average HD, and average size of

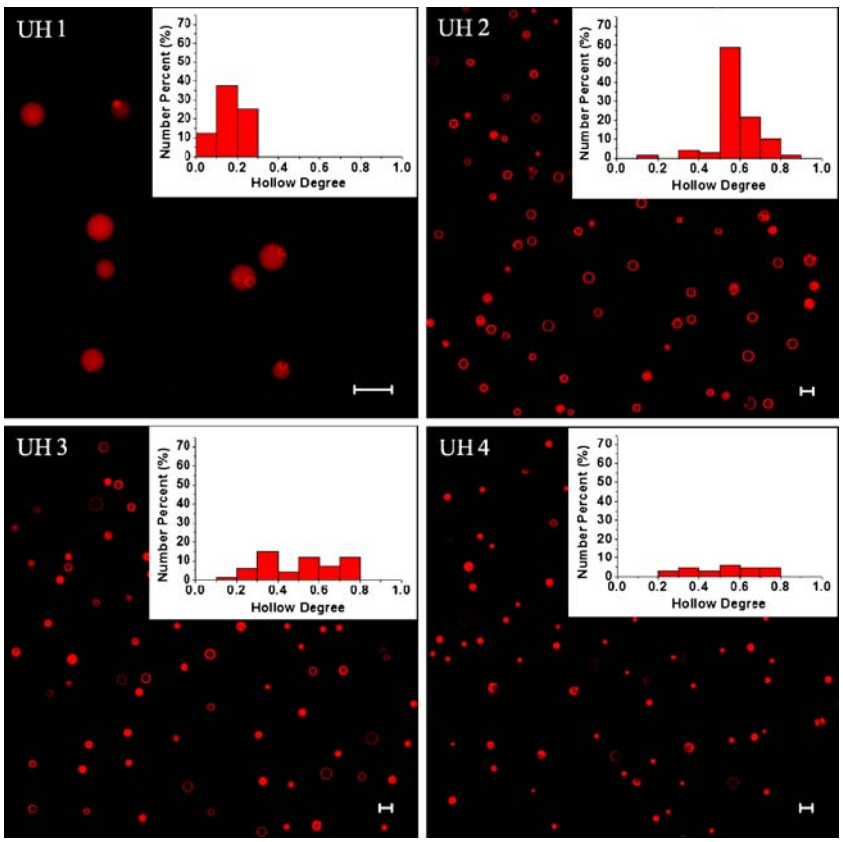

Fig. 3 LCSM images of UH series microcapsules prepared by different W_1/O volume ratios (UH represent that the first and second emulsification are by ultrasonic and homogenizer, respectively. The W_1/O volume ratios, for example *UH1* to *UH4*, are 0.1, 0.2, 0.4, and 0.5, respectively. The *insets* are number percent distributions of hollow degree. *Scale bars* represent 10 μm in all of images)

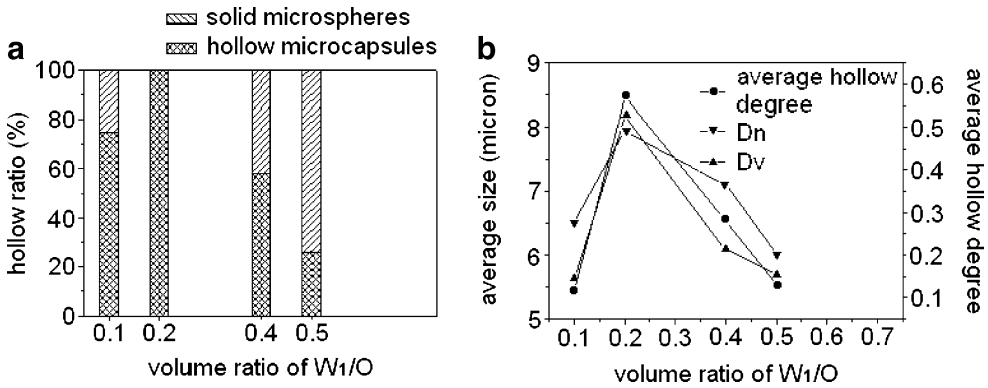

Fig. 4 **a**, **b** Influence of W_1/O volume ratio on the hollow ratio, average hollow degree and average size of microcapsules using ultrasonic in the first emulsification (D_n and D_v represent the number average size calculated from LCSM images and the volume average size measured by laser granulometry, respectively)

microcapsules increase first and then fall down with the raise of W_1/O volume ratio. The similar characteristic of UH series samples to HH series samples indicate again the important role of W_1/O volume ratio in controlling the hollow structure of microcapsules as well as the intrinsic relationship between size and HD.

With the increase of W_1/O volume ratio, the similar variational tendency of inner structure appeared in HH and UH series samples can be rationalized by considering the mechanism for the formation of double emulsion, which is shown in Scheme 2. On the condition of a small volume of W_1 is applied, the aqueous droplets in the first W_1/O emulsion would be scarce and small. During the second emulsification, many oil droplets cannot catch any aqueous droplets; as a result, those oil droplets become solid microspheres after solvent evaporation, while other oil droplets that have caught small aqueous droplets will become hollow microcapsules with low HD (Scheme 2a). With the increased volume of W_1, aqueous droplets in the first W_1/O emulsion would become more and bigger. More and more oil droplets can catch bigger aqueous droplets (Scheme 2b), so that the HR and average HD of resultant microcapsules will be improved accordingly. When the volume ratio of W_1/O gets to an optimal proportion, the resultant microcapsules will possess a high HR and average HD, like sample HH6 or UH2. Afterwards, further increasing the volume of W_1 will result in the further increase of specific area of W_1. Due to the hydrophobicity of PLLA, large specific area of W_1 will cause the precipitation of PLLA on the W_1/O interface, which will destroy the structure of resultant microcapsules (Scheme 2c). This deduction was confirmed by our observation during the experimental process, i.e., the W_1/O emulsion was no longer well liquid, and the damaged microcapsules were observed in HH7 and HH8.

In addition to the influence on HR and average HD, W_1/O volume ratio also affects the average size of microcapsules. The intrinsic relationship between size and HD can be illustrated in Scheme 3. With the evaporation of methylene chloride in O, PLLA macromolecular chains gradually close to the inner aqueous droplet. If there are two oil droplets with the same outer diameter but with different size of aqueous droplet inside, after methylene chloride evaporates completely, the resultant microcapsule with a small aqueous droplet inside (Scheme 3a) will be smaller than the one with a big aqueous droplet inside (Scheme 3b). That is why the solid microspheres are normally smaller than the hollow microcapsules in the LCSM images.

Comparing Figs. 2a and 4a, when the W_1/O volume ratio is 0.2, HH2 has lower HR than that of UH2. In other words, only small volume of W_1 is needed to achieve a high HR for UH series. For elucidating this result, it is considered

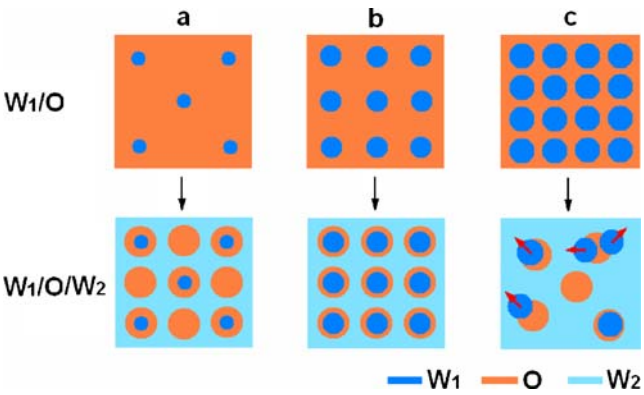

Scheme 2 Mechanism for the key effect of W_1 on the formation of double emulsion

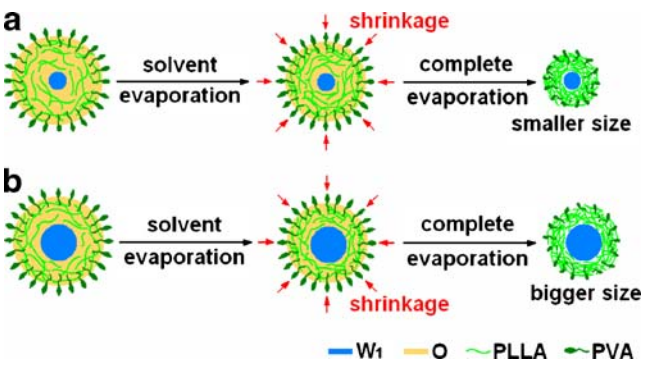

Scheme 3 The size of inner aqueous droplets influence the size of resultant microcapsules

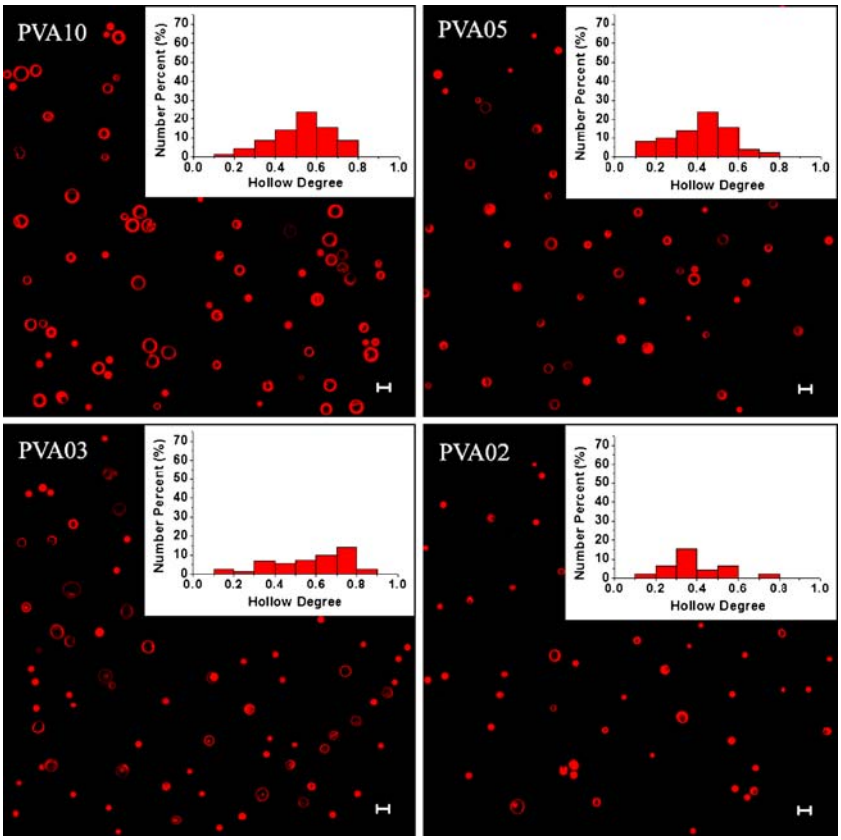

Fig. 5 LCSM images of microcapsules prepared at different PVA concentrations (*PVA10*, *PVA05*, *PVA03*, and *PVA02* represent that the PVA concentration are 1.0, 0.5, 0.3, and 0.2 wt. %, respectively. The *insets* are number percent distributions of hollow degree. *Scale bars* represent 10 μm in all of images)

that ultrasonic can break W_1 into much smaller aqueous droplets which can be captured entirely by oil droplets during the second emulsification. However, the energy of homogenizer is lower than that of ultrasonic so that homogenizer cannot break W_1 into aqueous droplets as smaller as the ultrasonic does. Those big aqueous droplets cannot be captured by oil droplets during the second emulsification, which cause the lower usage of W_1 and, therefore, the low value of HR in product. In addition, comparing two samples with near 100% HR, UH2 possess obvious smaller inner cavities than that of HH6. This result approves that ultrasonic can break W_1 into smaller aqueous droplets which is used as the precursor of inner cavities of the resultant microcapsules.

The second emulsification

The objective of the second emulsification is to obtain $W_1/O/W_2$ double emulsion. Since W_2 is used as continuous phase, its volume has little effect on the size and hollow structure of resultant microcapsules [36]. Whereas the concentration of PVA aqueous solution and the energy of the second emulsification are considered to play important roles during the second emulsification, since PVA is important for stabilizing the $W_1/O/W_2$ structure [37] and the emulsification energy will greatly affect the size of disperse phase (W_1/O emulsion). So for the second emulsification, we take PVA concentration and emulsification energy as two important parameters and studies their effect on the resultant microcapsules.

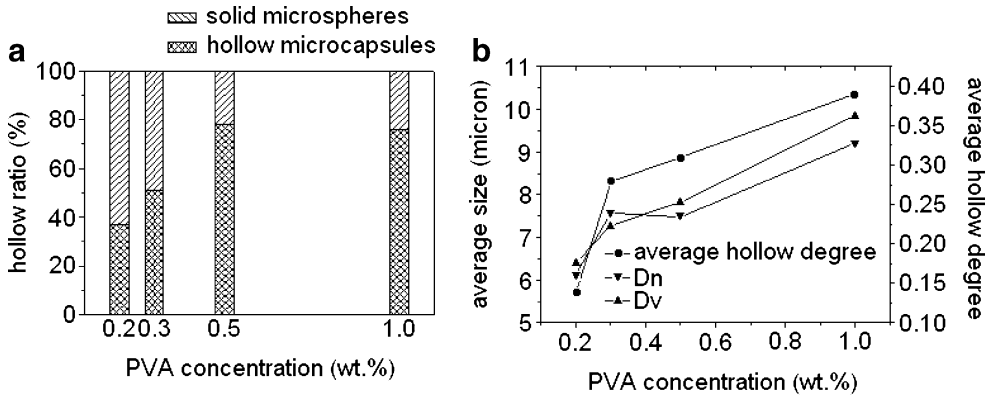

Fig. 6 **a**, **b** Influence of PVA concentration on the hollow ratio, average hollow degree and average size of microcapsules (D_n and D_v represent the number average size calculated from LCSM images and the volume average size measured by laser granulometry, respectively)

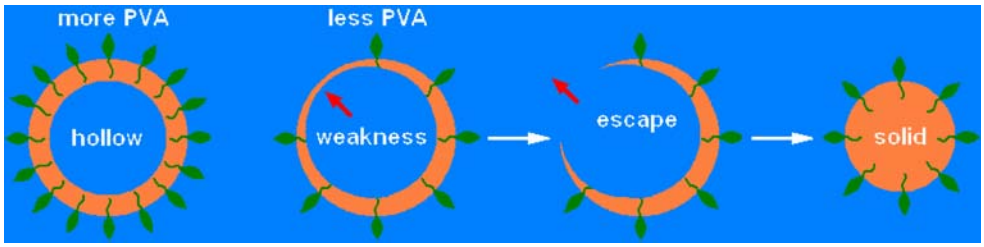

Scheme 4 Mechanism for the influence of PVA concentration on the hollow structure of microcapsules

In order to evaluate the influence of PVA concentration on the size and hollow structure of microcapsules, concentration from 1.0 to 0.2 wt.% in PVA aqueous solution were applied to fabricate microcapsules. The LCSM images of resultant microcapsules and their number percent distributions of HD are shown in Fig. 5. It is obvious that with the decrease of PVA concentration, more solid microspheres appear along with number percent distribution of HD moved to the lower value. There are few hollow microcapsules observed at the PVA concentration of 0.2 wt.%. Figure 6a shows the HR of each sample which decrease gradually with the decrease of PVA concentration.

The explanation for this result is clarified by Scheme 4. In $W_1/O/W_2$ double emulsion, PVA is used for stabilizing the $W_1/O/W_2$ structure. When there are less PVA molecules between O and W_2, osmotic pressure will compel the inner aqueous droplet to escape from the oil droplet through the weak part of oil film. Then, the $W_1/O/W_2$ structure will be broken and transform into simple O/W_2 structure. This transformation happens frequently at lower concentration of PVA; as a result, more solid microspheres are obtained. Since PVA molecules play an important role in the stability of $W_1/O/W_2$ structure, it is necessary to seek a suitable PVA concentration for fabricating microcapsules and insuring high HR in product.

The average HD and average size of microcapsules prepared at different PVA concentrations are shown in Fig. 6b, where they decrease gradually with the decrease of PVA concentration. The same variational tendencies reveal again the intrinsic relationship between size and HD, which has already been illustrated in Scheme 3.

Generally speaking, in simple emulsion, the size of disperse phase will increase as the concentration of emulsifier in the continuous phase decreases [33]. However, a reverse regularity was displayed in Fig. 6b. It is considered that the size of microcapsules mainly relates to their inner structures. As interpreted in Scheme 3, if an oil droplet has an aqueous droplet inside, the resultant microcapsule will be bigger than the one formed by the oil droplet that without any aqueous droplet inside. When the PVA concentration decreases, more and more $W_1/O/W_2$ structures transform into simple O/W structures, and solid microspheres are obtained, accompanied by the decrease of particle size.

The emulsification energy is another vital parameter during the second emulsification [33]. To our knowledge, no report until now focused on its influence on the inner structure of microcapsules prepared by $W_1/O/W_2$ double emulsification. Here, different emulsification energies are applied during the second emulsification for further investigation. As displayed by the LCSM images in

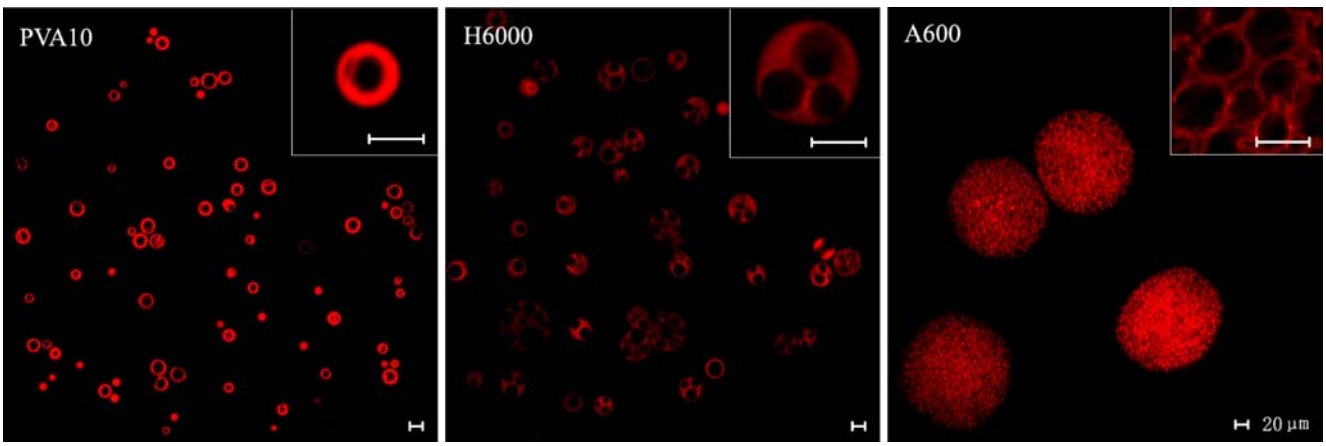

Fig. 7 LCSM images of microcapsules with single cavity or multi-cavities (the approach of the second emulsification for sample *PVA10*, *H6000*, and *A600* are 11,000 rpm homogenizer, 6,000 rpm homogenizer, and 600 rpm mechanical agitation, respectively. The *insets* are amplificatory images. *Scale bars* represent 10 μm except for the *marked* one)

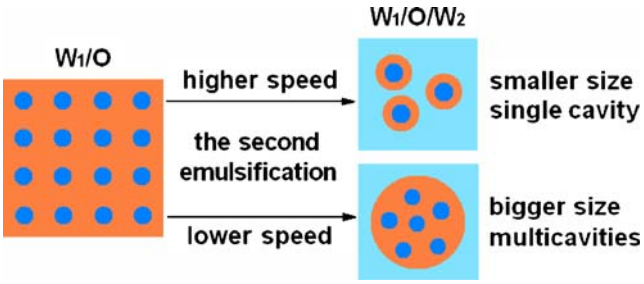

Scheme 5 Microcapsules with different hollow structures are obtained by varying the energy of the second emulsification

Fig. 7, with the emulsification energy decreasing from 11,000 to 6,000 and then 600 rpm, the microcapsules vary not only in size but also in their inner structures, i.e., the size increases and the inner structure changes from single cavity to multicavities. Besides, it is interesting to find that the capsules formed by different energy of the second emulsification possess similar size of inner cavities, as shown in the insets of Fig. 7. This result can be rationalized by Scheme 5. During the second emulsification, different energies cause the variation in size of oil droplets. Smaller oil droplets catch few aqueous droplets, even only one droplet at 11,000 rpm, thus, causing the formation of single cavity. With the decrease of emulsification energy, the resultant bigger oil droplets can catch several or much more aqueous droplets, which cause the formation of multicavities or even honeycomb structure.

Acoustic properties and inner characteristics

UCAs produce contrast imaging through altering the acoustical properties of tissues. Those acoustical properties include back scattering signals, nonlinear harmonic, sound attenuation, phase velocity, and so forth. Ultrasound parametric imaging from sound attenuation is a new technique for ultrasonic imaging, which is helpful for tissue characterization and diagnosis of early non-occupancy canceration [38]. Here, sound attenuation spectra and resonant frequencies of microcapsules with different hollow structures are measured to reveal the influence of hollow structures on the acoustical properties of microcapsules.

Images shown in Fig. 8a to d are sound attenuation spectra, hollow structures, and size distributions for sample UH1 and UH2. In the sound attenuation spectrum of sample UH1, an obvious peak appears at the incident frequency around 1 MHz, and the shape is acute and narrow. While for sample UH2, a smooth and wide peak appears around 2.5 MHz. As we know, when the incident frequency nears the resonance frequency of microcapsules, effective absorption of ultrasonic energy will be observed. From the sound attenuation spectra in Fig. 8, we estimate that the resonance frequency for sample UH1 and UH2 are 1.1 and 2.6 MHz, respectively. Resonant frequency depends on shell properties, shell thickness, and bubble size of the balloons. At the same shell materials and constant shell thickness, the resonant frequency will increase with decreasing bubble size. Comparing two samples investigated, UH1 has the smaller bubble size but the thicker shell. The cooperative effect of bubble size and shell thickness on the resonant frequency result in the resonant frequency of UH1 to be lower than that of UH2.

After dry powder microcapsules are dispersed in water, whether they are air-filled or water-filled will directly affect the capability of application. The acoustical test can indicate the air-filled nature of microcapsules and we also

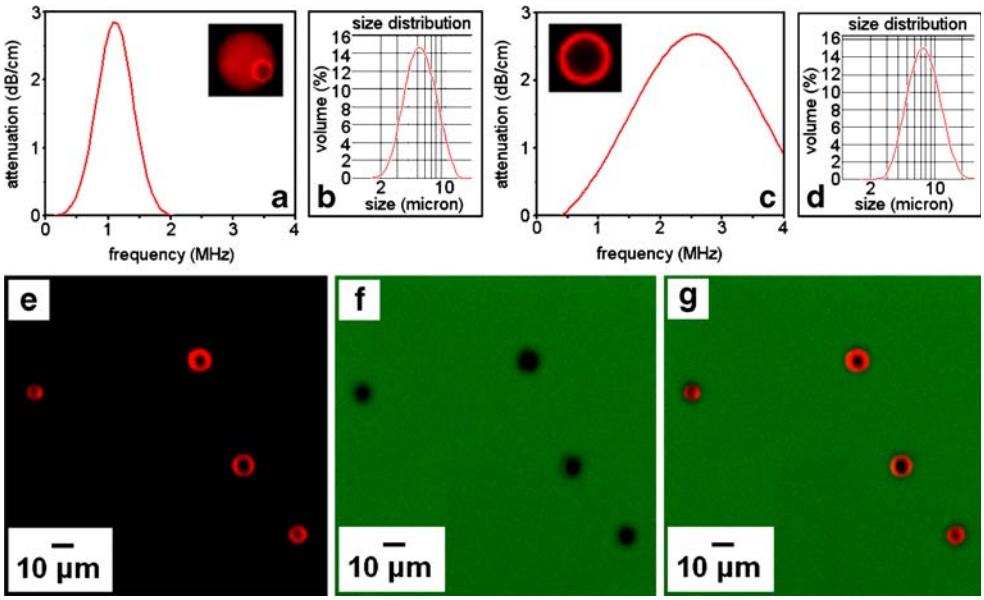

Fig. 8 Sound attenuation spectra of microcapsules with different hollow structures and size distributions and the LCSM images of rhodamine-marked microcapsules dispersed in fluorescein sodium salt–marked water (**a** and **b** sample UH1, **c** and **d** sample UH2, **e** 543 nm channels, **f** 488 channels, **g** combined **e**/**f** images)

have another direct way to confirm by using the so-called double fluorescence guide mark (DFGM). For DFGM, microcapsules are dispersed in water marked by hydrophilic green fluorescence dye. If water could enter into the capsules, green fluorescence would be observed in the cavities under confocal microscopy. On the contrary, the inner space of the capsules would be dark. As shown in Fig. 8e–g, the experimental result confirmed the air-filled nature of the microcapsules we fabricated. It is considered that the gas impermeability of microcapsules depends on the hydrophobicity of PLLA shell.

Conclusions

We present an efficient fabrication of PLLA microcapsules by an improved double emulsion–solvent evaporation technique. Considering the importance of hollow structure, concepts of HR and HD were introduced to quantitatively characterize the hollow structure of microcapsules. Detailed studies indicated that the volume ratio of inner aqueous phase (W_1) to middle oil phase (O) was a vital parameter for preparing high HR product. Neither too high nor too low W_1/O volume ratio was favorable to the output of hollow microcapsules. Besides, a suitable concentration of emulsifier in the outer aqueous phase (W_2) was the guarantee for a high HR as well. Moreover, the size of microcapsule was found to have great relationship with its HD. It was also revealed that the energy of both first and second emulsification would influence the hollow structure of microcapsules. Bigger microcapsules with multicavities inside could be obtained at a lower energy of the second emulsification. In addition, in the second emulsification, increasing the speed of homogenizer, or prolonging the time of emulsification can decrease the size distribution of balloons effectively. In order to explore the application in ultrasonic imaging, the sound attenuation spectra of polymeric microcapsules were measured, and it is revealed that microcapsules with different hollow structures had distinct sound attenuation spectrum and resonance frequency. These acoustic results demonstrate that it is possible to adjust the ultrasonic properties of UCAs by varying the hollow structure of microcapsules.

Acknowledgments This work was financially supported by *National Natural Science Foundation of China* (Project No. 30600751 and 30772349) as well as *Science and Technology Committee of Shanghai* (Project No. 05XD14015). We thank Instrumental Analysis Center of Shanghai Jiao Tong University for the help in characterization.

References

1. Klibanov AL (1999) Adv Drug Delivery Rev 37:139
2. Unger EC, Hersh E, Vannan M, McCreery T (2001) Echocardiogr 18:355
3. Mayer RC, Bekeredjian R (2008) Adv Drug Delivery Rev 60:1177
4. Van Liew HD, Burkard ME (1995) J Appl Physiol 79:1379
5. Van Liew HD, Raychaudhuri S (1997) J Appl Physiol 82:2045
6. Sukhorukov GB, Rogach, AL, Zebli B, Liedl T, Skirtach AG, Kohler, K, Antipov AA, Gaponik N, Susha AS, Winterhalter M, Parak WJ (2005) Small 1:194
7. Sboros V (2008) Adv Drug Delivery Rev 60:1117
8. Borden AM, Zhang H, Gillies JR, Dayton AP, Ferrara WK (2008) Biomaterials 29:597
9. Blomley MJK, Cooke JC, Unger EC, Monaghan MJ, Cosgrove DO (2001) Brit Med J 322:1222
10. Pisani E, Tsapis N, Paris J, Nicolas V, Cattel L, Fattal E (2006) Langmuir 22:4397
11. Ophir J, Parker KJ (1989) Ultrasound Med Biol 15:319
12. Andrew PM, Navin CN (2004) Ultrasound Med Biol 30:425
13. Cui WJ, Bei JZ, Wang SG, Zhi G, Zhao YY, Zhou XS, Zhang HW, Xu Y (2005) J Biomed Mater Res B 73:171
14. El-Sherif MD, Wheatley AM (2003) J Biomed Mater Res A 66:347
15. Straub JA (2005) J Control Release 108:21
16. Cui W (2005) J Biomed Mater Res B 73:171
17. Cheng S, Dy TC, Feinstein SB (1999) Am J Cardiol 81:41
18. Mor AV, Robinson K, Schroff S (1994) J Am Soc Echocardiog 7:29
19. Uhich KE, Cannizzaro SM, Langer RS, Shakesheff KM (1999) Chem Rev 99:3181
20. Klibanov AL (1999) Adv Drug Delivery Rev 37:139
21. Yeo Y, Back N, Park K (2001) Biotechnol Bioeng 6:213
22. Jain AR (2000) Biomaterials 21:2475
23. Zhu HG, McShane JM (2006) Chem Commun 2006:153
24. Vrancken NM, Clays AD (1970) US Patent 3,526,906
25. Jaeger CN, Trvernier HB (1971) British Patent 1,405,108
26. Ogawa Y, Yamamoto M, Takada S, Okada H, Shimamoto T (1998) Chem Pharm Bull 36:1502
27. Liu R, Huang SS, Wan YH, Ma GH, Su ZG (2006) Colloid Surface B 51:30
28. Koo YH, Chang TS, Choi SW, Park JH, Kim DY, Velev DO (2006) Chem Mater 18:3308
29. Cheng JJ, Teply AB, Sherifi I, Sung J, Luther G, Gu XF, Levy-Nissenbaum E, Radovic-Moreno FA, Langer R, Farokhzad CO (2007) Biomaterials 28:869
30. Xie SY, Wang SL, Zhao BK, Han C, Wang M, Zhou WZ (2008) Colloids Surf B Biointerfaces 67:199
31. Cavalieri F, Hamassi EA, Chiessi E, Paradossi G (2005) Langmuir 21:8758
32. Gong YJ, Zhang D, Gong XF, Tan KB, Liu Z (2006) Chinese Phys 15:1526
33. Lu R, Dou HJ, Sun K (2008) Chem J Chinese U 29:1176
34. Graaf van der S, Schroen CGPH, Boom MR (2005) J Membrane Sci 251:7
35. Lassalle V, Ferreira LM (2007) Macromol Biosci 7:767
36. Liu R, Ma GH, Meng FT, Su ZG (2005) J Control Release 103:31
37. Kanouni M, Rosano LH, Naouli N (2002) Adv Colloid Interfac 99:229
38. Lindner RJ (2004) Nature 3:527